APPENDIX C

Aeroacoustics of a High Aspect-Ratio Jet

APPENDIX C

Aeroacoustics of a High Aspect-Ratio Jet

Scott E. Munro*
and
K. K. Ahuja
Georgia Institute of Technology
GTRI/ATASL
Atlanta, GA, 30332-0844

Abstract

Circulation control wings are a type of pneumatic high-lift device that have been extensively researched as to their aerodynamic benefits. However, there has been little research into the possible airframe noise reduction benefits of a circulation control wing. The key element of noise is the jet noise associated with the jet sheet emitted from the blowing slot. This jet sheet is essentially a high aspect-ratio rectangular jet. Thus, to fully understand the noise of a circulation control wing, the noise of high aspect-ratio rectangular jets must also be understood. A high aspect-ratio nozzle was fabricated to study the general characteristics of high aspect-ratio jets with aspect ratios from 100 to 3000. The jet noise of this nozzle was proportional to the 8^{th} power of the jet velocity. It was also found that the jet noise was proportional to the slot height to the 3/2 power and slot width to the 1/2 power.

Nomenclature

A -- Area (typically of nozzle)
AR -- Aspect ratio
a -- Speed of sound
a_o -- Ambient speed of sound
D -- Diameter of round jet exit
d_{eq} -- Equivalent diameter, $2(A/\pi)^{1/2}$
f -- Frequency
HARN -- High aspect-ratio nozzle
h -- Slot height or rectangular nozzle height (small dimension)
I -- Sound intensity
L -- Characteristic length
L_{eq} -- Characteristic length for the HARN, $L_{eq} = h^{3/4}w^{1/4}$
M_c -- Convection Mach number
P -- Sound power
P_{ref} -- Reference acoustic pressure, 20 μPa
p -- pressure
R -- Radial distance from jet exit to measurement location
Re -- Reynolds number
SPL -- Sound Pressure Level
w -- width of rectangular nozzle (large dimension)
V_j -- Jet exit velocity (fully expanded)
Θ -- Angle of measurement with respect to the flow axis
ρ -- density

Introduction

Motivation

Circulation control wings (CCW) have been researched and developed extensively, primarily for the purpose of greatly increasing lift while reducing or replacing the conventional flap system of an aircraft. More recently CCW have been considered as a possible option for reducing airframe noise. However, there are many issues that need to be resolved. The acoustic effects of many parameters must be investigated, such as the slot height and width, and slot blowing velocity. In order to correctly define the best combination, new areas of research will have to be investigated, including high aspect-ratio rectangular jet noise. This was the motivation of the present study.

The CCW slot jet essentially creates a high aspect-ratio jet, but little research has been performed on high aspect-ratio jet noise, particularly on the very high aspect ratio of a CCW. Thus, this study was devoted to determining the general acoustic characteristics of high aspect-ratio rectangular jets, providing a basic level of understanding that could then be extended to other applications, in particular the CCW case.

Background

Since there has been little work on high aspect ratio rectangular jet noise, particularly aspect ratios applicable to a CCW, the following sections highlight literature on jet noise for both round and rectangular nozzles.

Jet Noise from Round Nozzles

As soon as jet and rocket engines began making their way into the aircraft designs, the noise from these new types of engines became an issue. In some cases it was more for controlling damage, such as in the case of a rocket launch, where the launch

* Now works for the Naval Air Warfare Center, Weapons Division, China Lake, CA 93555-6100

area is subjected to a large amount of noise from the rocket motors during the launch. The other major issue came with increased jet travel and jet aircraft activity around airports. The new jet aircraft were much louder and more annoying to the surrounding population.

Thus, research into jet noise soon began to emerge. Much of the early theoretical gains in jet noise prediction came from Lighthill's work on round jets. Various versions of this work are found in references [1- 3]. Lighthill suggested that the noise associated with a particular eddy could be represented by a quadrupole source. From this physical model, several relationships were derived, including 'Lighthill's eighth power law' relationship for the sound intensity[1-4]

$$I \sim \frac{\rho_m^2 V_j^8 D^2}{\rho_o a_o^5 R^2}(1 - M_c \cos(\Theta))^{-5} \quad (1)$$

There are important relations that are shown, specifically that the sound intensity is proportional to the eighth power of velocity and inversely proportional to the square of the radius between the source and observer. In the equation, Θ is the angle of the observer with respect to the downstream jet axis.

The frequency of the noise is also affected by test conditions. Near the exit of the nozzle where the mixing region is small, the turbulence is dominated by small eddies, thus higher frequency noise is associated with the small length scale. As the shear layer grows, the larger eddies further downstream are believed to be responsible for lower frequency jet noise.[4,-6] But notice that these characteristics are dependent on the geometry and mixing characteristics of the jet. Thus, the frequencies must also scale in order to be able to predict the entire spectrum of jet noise. The frequency scaling is taken into account by non-dimensionalizing the frequency into a Strouhal number and accounting for the moving sources. This non-dimensional frequency is typically expressed as:

$$\frac{fD}{V}(1 - M_c \cos\Theta) \quad (3)$$

Most of Lighthill's theory has been experimentally verified for unheated, subsonic, round jets. One key study in this area was performed by Lush[4] and another by Ahuja, and Ahuja and Bushell.[5, 6] Ahuja made careful measurements of jet noise for 3 different diameter round jets. Ahuja verified the data by scaling all his data to the same condition, which would collapse all the data if Lighthill's theory were correct. Converting to SPL and normalizing by "standard" conditions, equation (1) becomes

$$"s\tan dard" SPL = SPL - 10\log\left(\frac{V}{V_s}\right)^8 - 10\log\left(\frac{D}{D_s}\right)^2 + 10\log\left(\frac{R}{R_s}\right)^2 - 10\log(1 - M_c\cos\Theta)^{-5} \quad (3)$$

where the variables with an 's' subscript signify conditions of the "standard" case. Thus, any SPL measurement from a jet could be transformed, or scaled to the SPL for this standard case. In the reverse, the 'Standard SPL' data could be scaled using a geometry, distance, or velocity to predict what the noise would be in that case. Bushell and Ahuja's experimental data for unheated jets agreed with many of Lighthill's predictions but did not match in all cases.[5,6] It should be noted that all of this work was done for a round jet and therefore is limited in its ability to predict noise only for round nozzles.

Recently Lighthill's theories have come under much scrutiny and some other jet noise theories have come to the forefront. One of those theories has been put forth by Tam and several other researchers.[7-10] They suggest that there are two different noise mechanisms, one that is associated with the large scale turbulence and one with the fine scale turbulence.[7-9] Tam and Auriault also claim that these two mechanisms dominate the acoustic jet noise spectra in different regions of the polar arc. Specifically, large-scale turbulence noise dominates the spectrum at small polar angles, while the fine scale turbulence dominates the spectrum at higher polar angles.[7-9] References [7 and 8] describe two generic noise spectra, one for each type of noise. These generic spectra have been applied to a wide variety of jet noise data with reasonable success.[7-10]

It is apparent that even in the case of the well-studied round jet, there is still discussion of the appropriate theory and scaling. This is also true of other jet noise from non-round nozzles and more complex suppressor nozzles. This is particularly true in the case of rectangular jets where there has not been nearly the focus given to round jets. The following section discusses in some detail the differences found between the round jet case and rectangular jet case.

Jet Noise From Rectangular Nozzles

Although round nozzles dominated most of the applications where jet noise was of interest, there have always been some applications where a rectangular nozzle is more appropriate. Thus, there has also been some work on the topic of rectangular jet noise.

Almost all work on jet noise was conducted on round jets until there were applications where a

non-axisymmetric shape had advantages over an axisymmetric nozzle. The first rectangular nozzle work strictly for noise reduction appears to be performed by Tyler, et al.[11] Other applications were more thrust related. Rectangular nozzles produced better performance at higher Mach numbers in military aircraft tests.[12,13] However, the rectangular nozzles in these applications typically had aspect-ratios from 2 – 7.[14] These early studies were typically also limited to higher subsonic or supersonic Mach numbers.[15] Other examples of very early studies are Maglieri and Hubbard's work on jets of different aspect-ratio,[16] and Cole's work on high aspect-ratio slot-noise.[17] Maestrello and McDaid investigated slot jets with aspect-ratios from 5 to 20.[18] Gruschka and Schrecker[19] and Schrecker and Maus[20] investigated the noise emitted from high aspect-ratio slot jets with aspect-ratios similar to 100. One of the major motivations behind this work was the fact that jet velocity of rectangular jets decayed at a higher rate compared with round jets, thus resulting in a lower sound energy.[21] However, in all these works, high aspect-ratio referred to aspect-ratios typically at least an order of magnitude lower (sometimes two orders of magnitude) than the CCW jet of interest in the present work.[14,19,20]

The research on rectangular nozzles has produced some differing results. The acoustic power dependence of V_j^8 for round jets has been found by some researchers[18] while V_j^7 has been found by others.[15,20,22] The work documented in references [18,19] found that the jet velocity dependence was actually a function of the aspect ratio of the jet. The range of aspect ratios tested was from 30 to 120, and the velocity scaling function ranged from V_j^6 to V_j^7.

Ffwocs-Williams suggested in reference [22] that the exit geometry can affect the noise by an additional component he termed "lip noise." The lip noise radiates as a fluctuating force dipole source. Typically, the dipole source radiates noise proportional to V_j^6. Reference [14] speculated that this noise combined with the turbulent mixing noise produced the V_j^7 relationship found in their investigation.

Kouts and Yu[15] also noted that the peak frequency of the spectra only had a weak dependence on jet velocity. They also found that the rectangular jet seemed to have more high frequency content than circular jets. Also in contrast to round jets, researchers found that the peak frequency has a weak dependence on the nozzle height.[15,19,20] This was unexpected since round jet noise has a strong dependence on jet diameter and the nozzle height is considered the appropriate scale for the initial mixing region in rectangular jets.[15]

The region where the highest levels of noise are produced in a jet is in the mixing layer around the core region.[21] This is where the shear is very high, and the associated velocities are also at their highest. Well downstream, the flow evolves into a round jet flow, however the flow velocities are much lower than the exit condition and therefore do not radiate jet noise at comparable levels to the near exit region.[21] However, as with round jets there are many theories that have been proposed. In addition to studying round jets, Tam has investigated other nozzle shapes including rectangular jets. In his studies, he has limited his research to low aspect-ratio nozzles. His results indicate that rectangular jets are actually similar to round jets.[9,24-27] References [24-27] show Tam's fits do indeed agree well with the experimental data. This indicates that round jet noise and rectangular jet noise are actually very similar since both can be fit to one set of generic spectral curves.

As is evident by the variation in data and theories, there is still much to be investigated in the area of rectangular jet noise. The aspect ratios considered 'high' in the above discussion are typically one or two orders of magnitude lower than the typical aspect ratio of the nozzles of the present study. Thus, there is definitely a need to generate some clean, systematic very high aspect-ratio noise data so that theories can be extended to this realm.

Experimental Set-up

High Aspect-ratio Nozzle Design and Fabrication

The major design consideration used to develop the HARN was to minimize the internal noise that could propagate outside and contaminate the pure jet noise that was the object of the study. The most important step one can take to reduce internal noise is to keep the internal velocities low, and make smooth transitions in the flow path so there is no separated flow. In order to utilize the high-pressure air supply systems of the acoustic facilities at GTRI, the HARN had to be attached to a 4" diameter pipe flange face. Since it was desired to keep the exit geometry of the nozzle similar to that of the CCW model used in references [28 and 29], the 4" diameter inlet pipe was connected to a round-to-rectangular transition section with an exit area of 2.75" X 2.75". This had to expand to the exit geometry of 30" wide by 0.003" to 0.020" high. This produced a contraction ratio of 20-150 depending on the slot height. A contraction ratio on the order of 10 is usually adequate to maintain plenum-like conditions in most wind tunnels.[30] Thus, the upstream portion of the HARN was considered to be an adequate plenum for the slot nozzle. The low flow velocity associated with a plenum would ensure low levels of internal noise. Considerable care was taken

to ensure minimum internal noise in the design of the HARN. Further details of design considerations can be found in reference [29]

Due to a combination of many factors, including cost, the weight of the finished product, and machinability of the material, the HARN was fabricated from 5/8" thick aluminum plate. Figure 1 shows a schematic and photo of the HARN. The exit of the HARN was 30" X 0.25". The top and bottom of the exit were cut back at a 30-degree angle and drilled-and-tapped to receive screws to hold down knife-edge blades. These make the final opening of the HARN slot exit. Shims were placed underneath the knife-edges to vary the height of the slot exit.

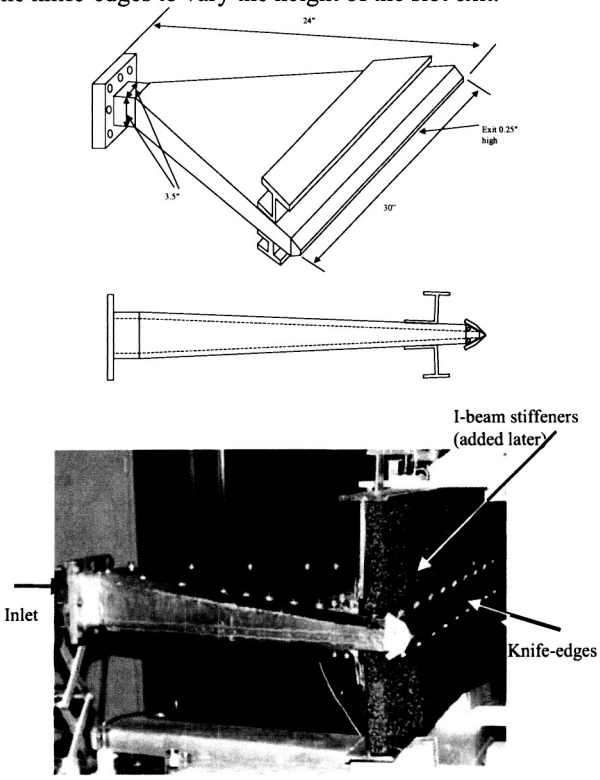

Figure 1: HARN Nozzle

The knife-edges were machined from steel for maximum strength. They were designed to create a converging nozzle for the flow and did not have a straight section parallel to the jet centerline. A straight section machined into the knife-edges would be a constant length. However, since the slot height varied greatly, the non-dimensional length of the straight section would vary significantly. Although it was believed that this would not change the acoustic characteristics of the flow, it was decided to eliminate any straight section to keep the flow characteristics similar for all nozzle heights.

Since one of the initial goals was to minimize internal noise, it was desirable to have no protrusions into the flow that might shed vortices and generate noise. Thus, no tie-down rods were used to help the HARN retain its shape under pressure. Under initial testing it was found that the top and bottom plates of the HARN would bow enough to generate as much as a 1/8" increase in nozzle exit height. This was unacceptable since this is an order of magnitude increase in the height. There were only two ways to resolve this issue, either add tie-down rods through the plenum interior to help carry some of the pressure load, or stiffen the top and bottom plates by adding stiffeners. It was felt that the risk of generating internal noise was too great to add tie-down rods to solve the problem. Thus, the decision was made to stiffen the top and bottom plate with stiffeners placed on the outside surface. Figure 1 shows the stiffeners installed on the HARN.

Some extra parts were also fabricated for additional tests. These included blanking plates that fit inside the HARN to block off portions of the nozzle, in order to test other jet widths. Three sets were made. These could be inserted inside the nozzle to reduce the width from 30" to 14.75" or 6.5". A much more detailed description of the HARN is provided in reference [29].

Instrumentation

The Cobb-County facilities of GTRI house two anechoic chambers, the anechoic static jet facility (ASJF) and an anechoic flight simulation facility (AFSF). The Acoustic data for the HARN could have been acquired in either of these facilities. However, due to scheduling with other projects the AFSF was used. Figure 2 shows a schematic of the HARN set-up in the AFSF. The facility itself has been described in detail references [28 29, and 31]. The facility consists of a converging duct that terminates as a 28-inch diameter round duct in an anechoic chamber. A collector extends out of the chamber on the opposite wall. Freestream flow is provided by a diesel powered fan on the downstream end of the collector. High-pressure air can be piped in through the center of the converging duct allowing for jet-flow and noise studies in the presence of a freestream. For these tests, the wind tunnel feature of the AFSF was not used, essentially making the facility a static test facility.

APPENDIX C

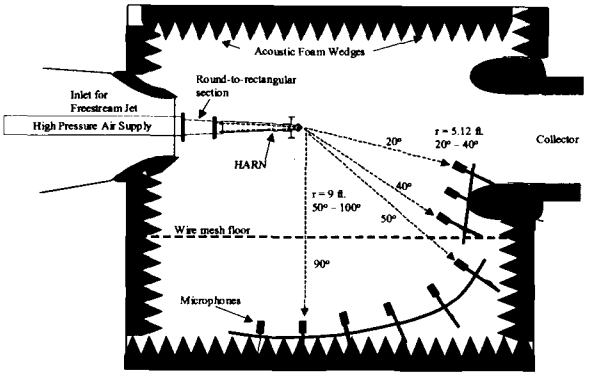

Figure 2: Schematic of HARN installed in AFSF.

Several microphones were placed on a polar arc at fixed angles. The microphone layout is shown in figure 2. More details can be found in reference [29]. Experience has shown that the response of the microphone system (microphone, pre-amplifier and extension cable) changes as the system ages. The microphones are commonly calibrated at one frequency, essentially to establish the conversion from output voltage to pressure amplitude. Unfortunately this assumes that the factory frequency response curve can be used to adjust this calibration over the entire frequency range. The only way to truly compare signals from different microphones is to calibrate the entire system over the entire frequency range of interest. The calibration was accomplished by using a noise source and a newly acquired microphone system as a reference at a reference location. The reference microphone signal was compared to the signal from each microphone. A frequency response correction was then generated for each microphone based on the difference between the reference and the corresponding microphone. More details about the frequency response calibration can be found in reference [29].

For the HARN acoustic tests, microphones were mounted at several angles with respect to the downstream jet axis, specifically, from 20° to 100° at 10° increments (0° being the jet axis in the downstream direction). Due to constraints of the facility (see figure 2), microphones at 20°, 30° and 40° had to be placed 5.12 feet from the nozzle exit, while the rest of the microphones were placed 9 feet from the nozzle exit.

All the microphones used in the tests were B & K type 4135 or type 3939 (replacement of 4135) microphones, with either B & K type 2669 or type 2619 preamplifier. The microphone/pre-amplifiers were connected to an HP 35650 Spectral Analyzer via B & K microphone extension cables and B & K NEXUS power supplies (with built-in conditioning amplifiers). Software based on a PC computer controlled the acquisition process and produced as outputs SPL versus frequency for each channel.

Critical flow and atmospheric parameters were monitored and recorded as necessary. The ambient pressure, temperature and humidity were recorded for each test point in order to make atmospheric absorption corrections to the acoustic data. The total and the ambient pressures were used to set specific exit pressure ratios, and hence jet exit Mach number. The total and static pressures and reservoir temperature were used to find the internal flow velocity. Details of these measurements and how the atmospheric absorption correction was applied are given in reference [29].

Acoustic Measurements Test Matrix

For each nozzle geometry, an attempt was made to acquire acoustic data at jet velocities of 500, 675, 785, 920, 1000, and 1100 ft/s. These corresponded to increments in total pressure that were relatively easy to achieve with the flow controls of the HARN.

A problem encountered when attempting to vary only one variable was that the slot height changed with increasing internal pressure. The knife-edges are attached only at one end and that the pressure exerted on the knife-edge causes a moment about the attachment point. Obviously, as the pressure is increased, the moment is increased and the tip deflects. It turned out that the deflection was even across the span, and seemed to be independent of the initial slot height. The increase in slot height due to this was found to be about 0.0015 in/psi. Unfortunately, for some of the smaller slot heights, this could double or even triple the height of the slot over the range of velocities tested, while causing a 50% increase in height for the larger initial slot heights. This caused a problem when trying to compare data for a constant slot height since the height changed for each velocity condition.

The nozzle width was changed by using blanking plates inside the nozzle. The width was variable from the full width of 30" to 15" and 6.5". These were installed by removing the top plate of the HARN and inserting blanking plates to the desired width.

Due to the extremely small nozzle heights and exit areas, precise jet velocities and slot heights were difficult to attain; however, a nominal test matrix was set. At each of the three nozzle widths mentioned above, a matrix of 4 slot heights and 5 jet velocities were tested. The initial slot heights were nominally 0.015", 0.030", 0.045", and 0.065". This produced aspect-ratios from as low as 100 to as high as 3000. At each slot height and width setting, acoustic data was acquired at 5 nominal jet velocity

conditions 500 ft/s, 675 ft/s, 785 ft/s, 920 ft/s, 1000 ft/s, and 1100 ft/s. At each test point (a particular w, h, and V_j) acoustic data were measured at 9 polar angles (20° – 100°) and the supporting pressure and temperature values were recorded as well.

Acoustic Measurements

Notes on Acoustic Measurements

High aspect-ratio jet noise data were acquired for several configurations of the HARN. The goal of the acoustic study was to try to determine the general acoustic characteristics of the very high aspect-ratio jet. An attempt was made to vary only one parameter at a time. However, as discussed in the previous sections, that often was not possible. Data will be presented as much as possible with only one parameter varying, and each variable's effect on far field noise spectra and overall sound pressure levels (OASPL) will be discussed. This enables an easy determination of a scaling factor for each variable. First however, it is beneficial to examine the general noise spectra associated with the HARN.

It should be noted that all acoustic data presented will be shown in 1/3-octave spectra or as OASPLs. The data were acquired in narrowband out to 80 kHz (Δf = 64 Hz) but the data were converted to 1/3 octave bands in order to make comparisons and references to the classic experiments[4-6] on subsonic round jets, which are only available in 1/3-octave bands. Also, all data presented here are corrected for several different factors to render the data lossless. These include corrections for the microphone grid, the presence of the microphone in the free-field, the absorption of sound due to the atmosphere, and the individual microphone frequency response correction. All of the corrections, except for the individual frequency response correction, were applied at the power spectral density levels. This was done to standardize the application of corrections that can vary depending on the bandwidth in which they are applied. These corrections are only mentioned here, details of the corrections and how they were applied to the data can be found in reference [29].

Typical Acoustic Data

The goal of the HARN acoustic test was to determine the general acoustic characteristics of an extremely high aspect-ratio nozzle. To accomplish this task, acoustic data were acquired at several jet velocities for a given nozzle geometry. There were a total of 72 test conditions, each with acoustic data at 9 polar angles. Since there is such a large amount of data, typical data for several conditions and polar angles will be presented in this section. Data at polar angles of 30°, 60° and 90° will be shown. Data at other polar angles can be found in reference [29]. One-third octave spectra will be presented for all velocities for a given nozzle condition.

Figure 3 shows the acoustic spectra for the 30" nozzle width. The figure shows typical data for the three polar angles for the initial slot height of 0.026". As with round jets, the lower polar angles have a more distinct peak in their spectra. There are also significant increases in the amplitude over the entire frequency spectrum as the velocity is increased. However, one cannot directly extract the velocity relationship from these plots since the slot height also increases as the velocity increases. It should also be noted that there is a small peak below 1 kHz in most of the spectra. This is believed to be associated with internal noise and this portion of the spectra will most likely not follow the trends associated with pure jet noise. The reader is advised to keep this in mind when examining the HARN data.

APPENDIX C

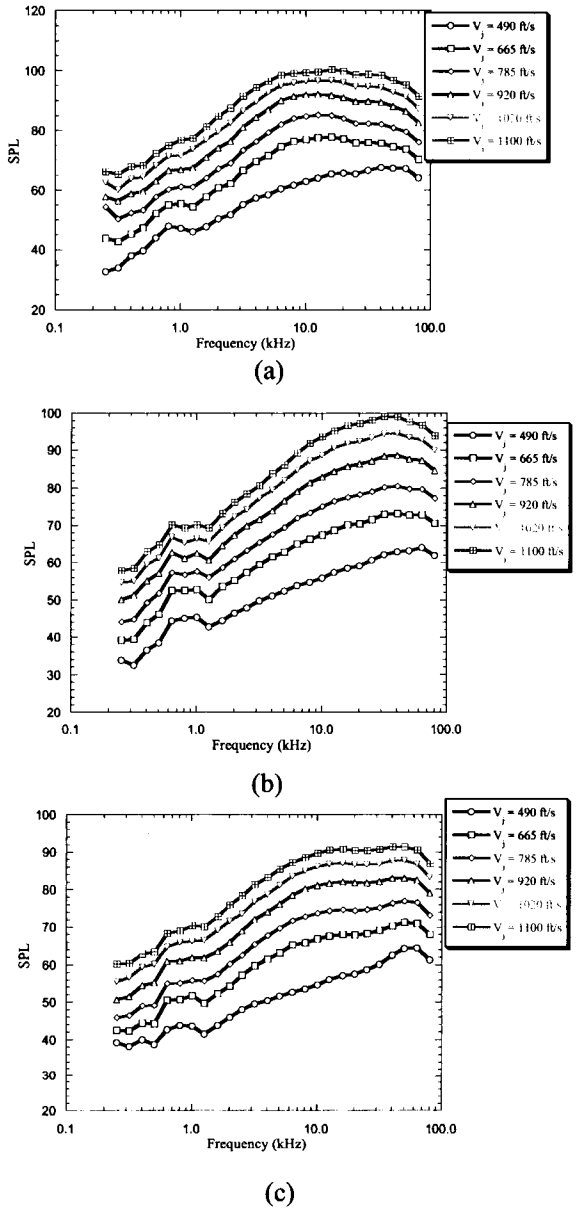

Figure 3: HARN acoustic data for h_o = 0.026", w = 30", (a) Θ = 30°, (b) Θ = 60°, (c) Θ = 90°.

Figures 4 and 5 show the data for the nozzle with widths set to 14.75" and 6.5", respectively. The corresponding initial slot heights were 0.039" and 0.048". Again, there is a more distinct peak for the 30° data, while the 90° data appear to have more of a flat spectrum. As with the 30" data, increased velocity causes large increases in the amplitude of the data. The 30° data peak frequency seems to increase with increasing velocity. The low frequency peak is also present in these figures. The low frequency peak is most likely due to internal noise, and should be ignored when using the HARN data. The data presented here are typical examples of the acoustic data for the HARN nozzle and are shown to present the general characteristics of the data.

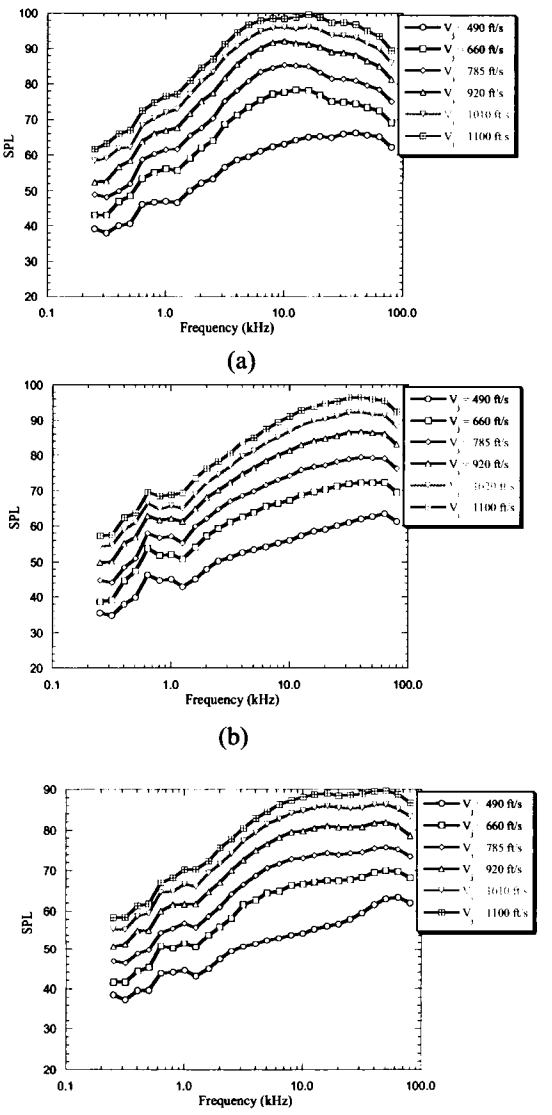

Figure 4: HARN acoustic data for h_o = 0.039", w = 14.75", (a) Θ = 30°, (b) Θ = 60°, (c) Θ = 90°.

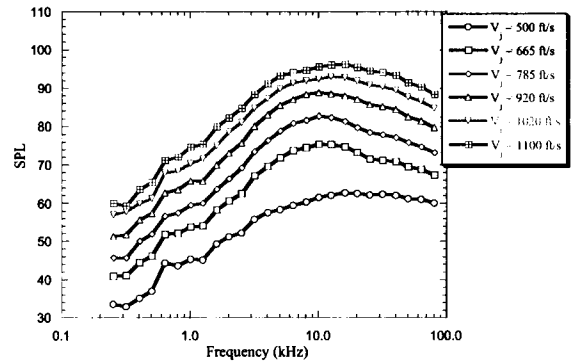

(a)

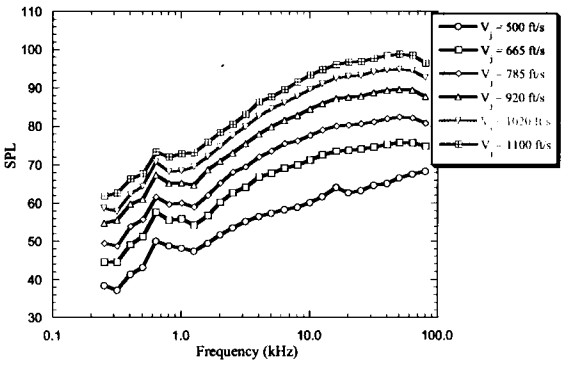

(b)

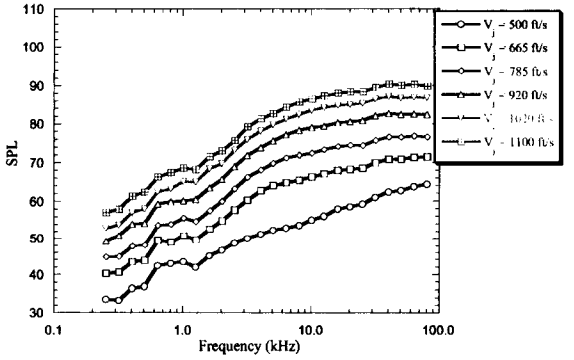

(c)

Figure 5: HARN acoustic data for h_o = 0.048", w = 6.5", (a) $\Theta = 30^o$, (b) $\Theta = 60^o$, (c) $\Theta = 90^o$.

In addition to variations in the spectra with nozzle geometry and jet velocity, the acoustic spectra varies depending on the polar angle where the data are acquired. Figure 6 shows acoustic spectra for a round jet from reference [6]. Notice that the SPLs increase at angles closer to the jet axis. There also is a larger amount of low frequency noise and there is some refraction of high frequency noise as well. These results are well established for the round nozzle.[5,6]

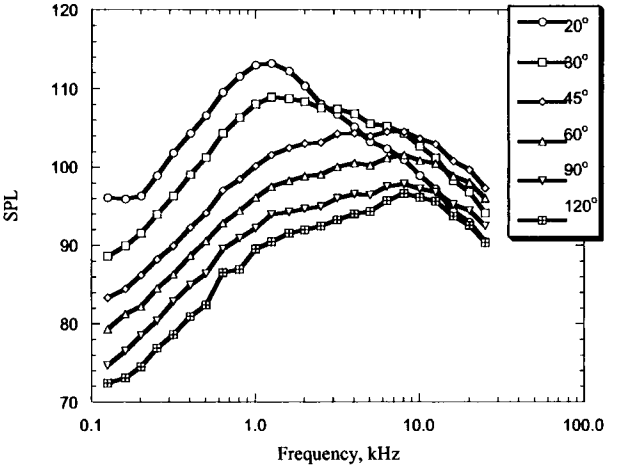

Figure 6: Round jet noise data for D = 2.4", V_j = 1000 ft/s, from reference [6].

Figure 7 shows similar data for the HARN. There are several differences that are noticeable. At first glance it appears that the spectral peak is at Θ = 40° for the HARN while it is closer to 20° for the round nozzle. However, if the low frequency data are closely examined, the 20° data are higher, indicating that in fact the peak directivity is closer to 20°. The lower spectral peak is most likely due to absorption and scattering of the noise due to turbulence. This effect was well documented in references [4], [5] and [6].

These spectra will be compared to acoustic data from other experiments later in this document. However, first it is desirable to determine how the acoustic amplitude changes due to changes in slot height, width, jet velocity and polar angle. An initial examination of these relationships will be performed in the next section using the OASPLs calculated from the data presented here.

APPENDIX C

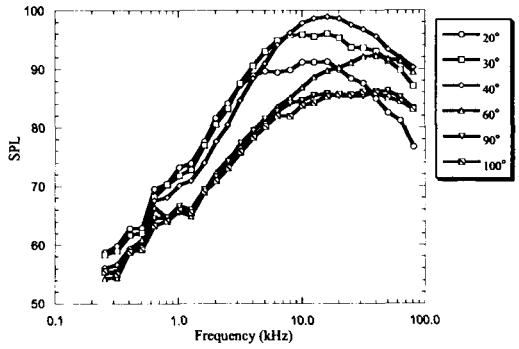

Figure 7: HARN jet noise data for w = 14.75", h = 0.057", V_j = 1010 ft/s.

Comparison of HARN Acoustic Data with Established Trends.

There has been very little experimentation with nozzles of high aspect-ratios. Most of the rectangular jet noise data available has been acquired for nozzles with aspect ratios below 20, while there is virtually no acoustic data available for nozzles with aspect ratios greater than 100. Lower aspect-ratio jet noise data has been compared successfully to round jet data by using an equivalent diameter as the geometric parameter.[9,26,27,32,33] There has been some discrepancy associated with the relationship between the SPL amplitude and the jet velocity. Some data has indicated a V^7 relationship while other data has shown a V^8 or even V^9 relationship.[15, 20, 32, 33]

Since round jet noise is essentially considered to be the standard to compare against and there is no accepted method for scaling rectangular jet noise, round jet noise data will be used as the standard for comparison and scaling of the HARN data. It has been well established that the OASPL for round a jet is proportional to V_j^8 and D^2 (if other variables are kept constant, such as density, speed of sound, etc.).[1, 2, 4, 5, 6, 34]

In addition to the geometry and the jet velocity, the amplitude of the acoustic spectra is dependent on the polar angle. Round jet theory shows that $SPL \sim (1-M_c\cos\Theta)^{-5}$. Experiments on round nozzles have found that this term alone is insufficient to completely collapse round jet noise data. It is believed that this is due to refraction and scattering of high frequency noise by the jet flow. This difference between the theory and the experimental data is shown in figure 8 where round jet noise from reference [6] is presented. Notice that the theory and the experimental data agree well at low jet velocity at all polar angles. However, the theory over-predicts the OASPL at higher jet velocity, especially in the rear arc.

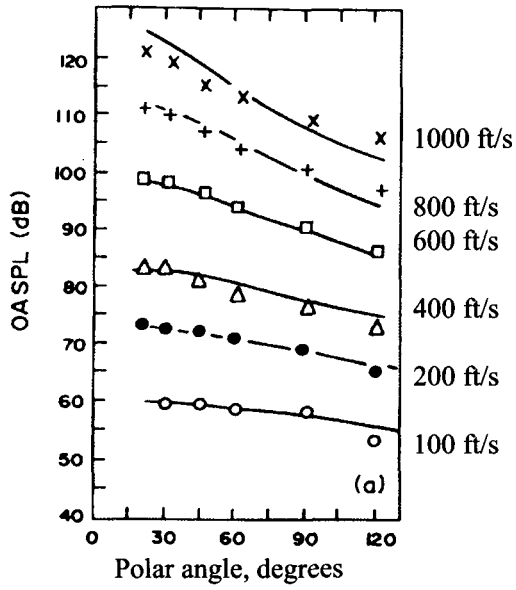

Figure 8: Directivities of OASPL's for round jet noise, D = 2.84", from reference [5].

OASPL was calculated for the HARN spectra over a frequency range from 1 kHz to 75 kHz. OASPL data are seen in figure 9 for the HARN. Notice that there is a greater difference between the theory and the data. At low jet velocities the theory predicts the amplitude reasonably well for angles greater than 40°. However, at very low polar angles there are significant differences and it is clear that the directivity does not follow the directivity given by $(1-M_c\cos\Theta)^{-5}$, even at low jet velocities. It is clear from figure 9 that the directivity given by $(1-M_c\cos\Theta)^{-5}$ does not appropriately represent the data. Thus, the following discussion will concentrate on data at the 90° polar angle to avoid the added complications of a polar angle effect.

APPENDIX C

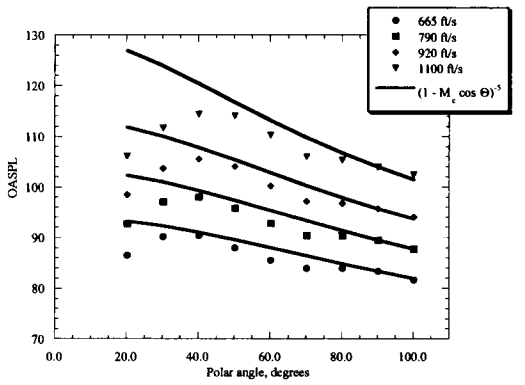

Figure 9: Directivities of OASPL's for HARN jet noise, w = 30", h_o = 0.04".

The equivalent diameter was also calculated using the measured slot height and width for each HARN test condition. The equivalent diameter is defined as

$$D_{eq} = (4A/\pi)^{1/2} = (4hw/\pi)^{1/2} \quad (4)$$

Thus, D_{eq} is dependent on square root of h and w. Figure 10 shows OASPL for HARN acoustic data plotted against the corresponding D_{eq} for constant jet velocity test conditions. As is obvious in the plot D_{eq}, is not the only parameter that determines the amplitude of the OASPL.

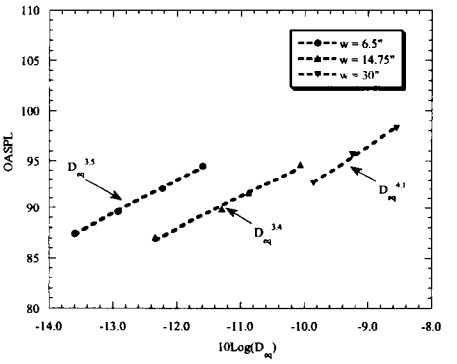

Figure 10: OASPL versus equivalent diameter for all the HARN data for constant V_j = 920 ft/s, Θ = 90°.

Figure 11 is a plot a plot of several HARN test conditions. Curves are shown for several nozzle widths. The OASPL change for a change in h only is shown since velocity and w are held constant for the points along each curve. As can be seen, the relationship between OASPL and h is not constant for all w, but a best fit to the data appears to be around $h^{3/2}$.

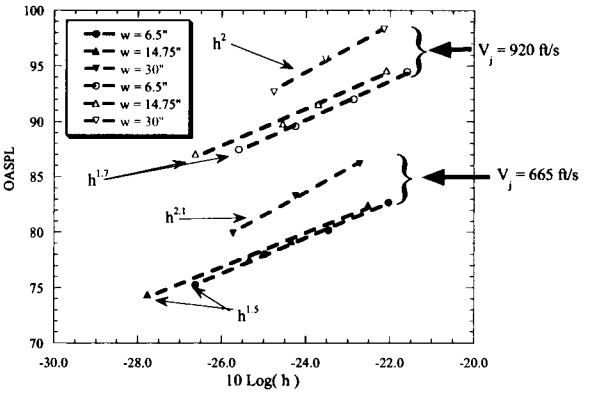

Figure 11: OASPL versus h for constant V_j and w, Θ = 90_o.

The OASPL data is plotted versus the jet velocity in figure 12. There are two things that can be quickly gained from this plot. First, the relationship between the OASPL and the jet velocity seems to be close to V_j^8. It should also be noted that the width also has a contribution to the OASPL. This can be seen by the fact that the h correction does not completely collapse all the data, only the data for constant w seem to fall along the same line.

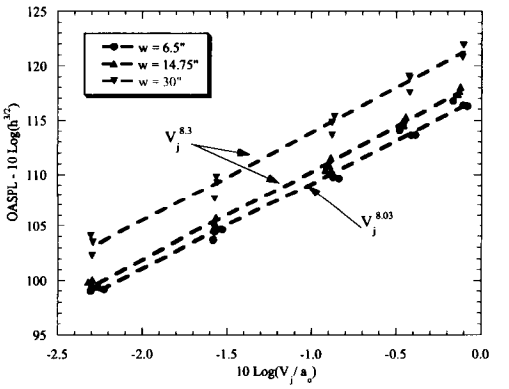

Figure 12: OASPL versus jet velocity for constant w, Θ = 90o.

Figure 13 shows the OASPL data plotted versus the width. Unfortunately there is not a distinct relationship that immediately appears from the plot, however a curve fit of the data does show a relationship following $w^{1/2}$ in the average.

APPENDIX C

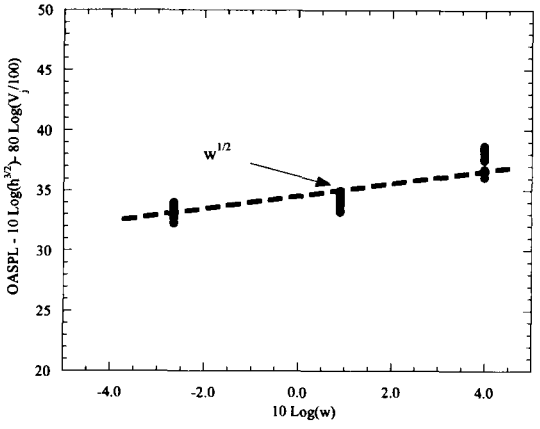

Figure 13: OASPL versus width, $\Theta = 90°$.

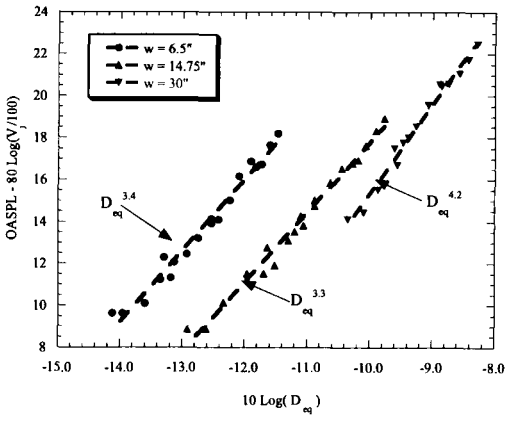

Figure 14: OASPL adjusted for jet velocity plotted versus equivalent diameter, $\Theta = 90°$

As was mentioned earlier, low aspect-ratio rectangular jet noise data is usually collapsed using an equivalent diameter.[7-9, 24-27] Now that the relationship for jet velocity is known, it can be used to derive a relationship for the equivalent diameter. Figure 14 shows OASPLs for a range of nozzle heights and widths plotted against equivalent diameter. This plot is similar to that shown in figure 10, except now the velocity component of the OASPL is subtracted out. There are some points that can be ascertained from this plot. Notice that there appear to be three sets of data points, each associated with a different nozzle width. It also should be noted that the OASPL is dependent on roughly the 4^{th} power of D_{eq} for constant w. This is contrary to typical scaling done for low aspect-ratio rectangular jets, which typically use the square of the equivalent diameter. If this were an appropriate way to scale the data, the data would have collapsed into one curve with the slope proportional to D_{eq}^2. Since this is not the case, the equivalent diameter is not an appropriate way to scale acoustic data for nozzles with aspect ratios as large as the HARN.

Several different schemes for collapsing jet noise data were used to try to determine an appropriate scaling. The HARN data does seem to follow the same trend as round jet noise does for jet velocity. However, the equivalent diameter does not satisfactorily collapse the data. A final attempt was made to collapse the data by simply using the data to determine relationships between the OASPL and nozzle width and height. No exact relationship can be extracted from figures 11 and 13 , however, a best fit to the data was found to be OASPL $\sim h^{3/2}w^{1/2}$. Incorporated into this determination was the desire to observe the noise intensity proportional to the square of a lengthy scale as derived by Lighthill, namely that $I \sim L^2$ for all else constant. Thus, to stay consistent with the length squared dimension, an equivalent length L_{eq} was defined as $L_{eq} = (h^{3/2} w^{1/2})^{1/2}$. Hence, OASPL $\sim L_{eq}^2$ for the HARN. Figure 15 shows the "best fit" to within +/- 1 dB for the HARN data and as expected the data collapses more tightly than any of the other schemes examined.

APPENDIX C

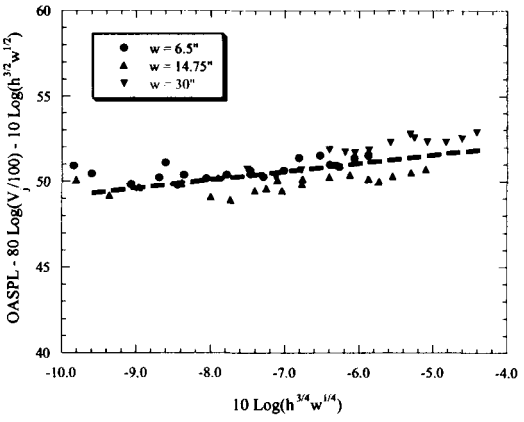

Figure 15: OASPL adjusted for area based on the "best fit" results found in the HARN study, $\Theta = 90^{\circ}$

In addition to the simple collapse using L_{eq}, an attempt was made to collapse the data using sliding exponents for h and w as the aspect-ratio changes. This was based on the expected relationships one would encounter at the extremes of the aspect-ratio range. At an aspect ratio of 1, one would expect the height and width to have equal contribution to the acoustic emissions. However, at extremely high aspect ratios, the height would be expected to dominate the acoustic emissions since the jet is essentially 2-dimensional. This sliding exponents of h and w relationship would better relate to the physical geometry of the flow, whereas the equivalent length defined here is more of an average length scale based on a wide range of geometric configurations. Unfortunately, a reasonable relationship using sliding exponents of h and w could not be found using only the three widths tested in the HARN experiments. Further exploration of this topic is left to future work.

In this short investigation of the OASPL of the HARN acoustic data several insights have been gained. It was found that the HARN noise intensity was not proportional to the square of D_{eq} as lower aspect-ratio rectangular nozzle data indicates. It was also found that the OASPL amplitude was proportional to V_j^8. This agrees with some of the research for rectangular nozzles as well as with the well-established results for round nozzles. In order to account for the discrepancy between the HARN data and low aspect-ratio data that is proportional to D_{eq}, the independent effects of h and w on the OASPL were sought. It was found that h and w appear to independently affect the OASPL data for the HARN. The OASPL appears to be proportional to $h^{3/2}$ and $w^{1/2}$.

The previous figures have all dealt with data at $\Theta = 90^{\circ}$. It is worthwhile to examine the relationships developed using the data at $\Theta = 90^{\circ}$ between the OASPL and h and w for different polar angles. Figure 16 shows data for several different geometric conditions at the same jet velocity scaled using the parameters found from the earlier figures. Notice that the corrected OASPL values tend to vary from one polar angle to another, but the points for a particular angle tend to collapse for many of the polar angles. Thus, it appears that the relationships for h and w are not functions of polar angle.

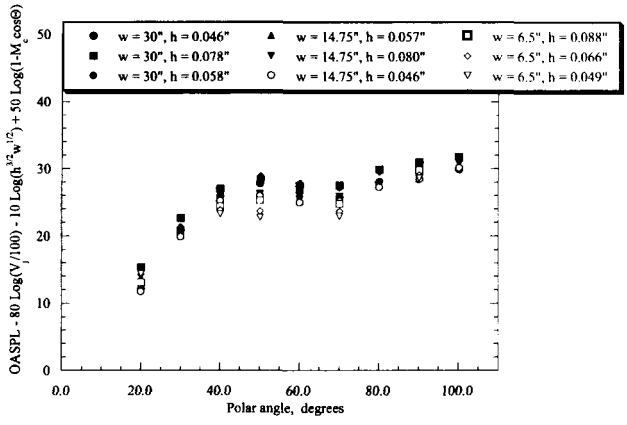

Figure 16: Directivities of HARN OASPL for several w and h combinations for constant $V_j = 1020$ ft/s.

Figure 16 showed that the OASPL relationships to h and w were consistent over most of the polar angles for a fixed jet exit velocity. Figure 17 shows a similar plot but now the jet velocity also varies. Notice that the spread of the data points, particularly at the lower angles, has increased. This indicates that OASPL ~ $V^8(1\text{-}M_c\cos\Theta)^{-5}$ is not the correct parameter for collapsing the data for all polar angles. This was somewhat expected since this result is similar to the round jet case, where this discrepancy is believed to be due to refraction and scattering of high frequency jet noise away from the low polar angles.[5]

APPENDIX C

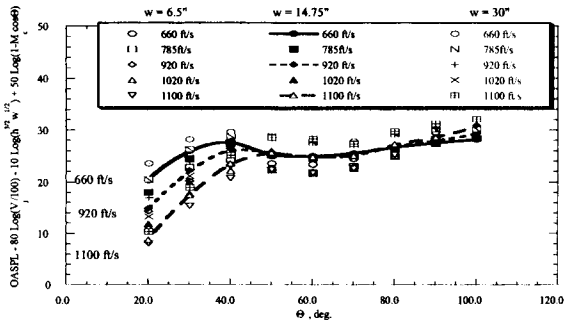

Figure 17: Directivities of HARN OASPL for various test conditions.

These same trends are evident not just in the OASPL for the HARN data, but also for the entire spectrum. Figure 18 shows several of the HARN spectra scaled by the jet velocity and the equivalent diameter. The frequency is also scaled by D_{eq} and by the Doppler term commonly used to account for the frequency shift due to the convecting eddies. Notice that this does not satisfactorily collapse the data, and in some frequency regions the spread is over 10 dB. It should be noted that this is the scaling found to be appropriate for round jets (at polar angles greater than 30°) and some low aspect-ratio rectangular jets. However, it is clearly not the proper choice for collapsing HARN data. Recall from figure 14 that the OASPL scaled with the amplitude corrected by D_{eq}^4 for constant width. Similar results are obtained if the spectra are examined, however, D_{eq}^4 again is not appropriate for collapsing spectra for different widths as was the case with the OASPL.

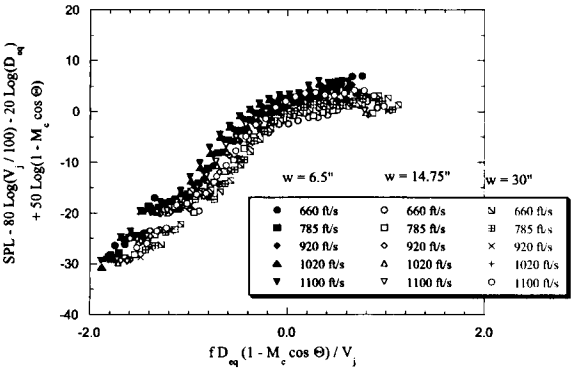

Figure 18: HARN acoustic spectra scaled using SPL ~ $V^8Leq^2(1 - Mccos\Theta)^{-5}$, $L_{eq} = h^{3/4}w^{1/4}$, $\Theta = 90°$.

Although these figures have shown that the data does collapse to some extent using the equivalent diameter as a scaling parameter, it definitely appears that it is not the best way to scale high aspect-ratio rectangular jet noise. The OASPL indicated that h and w have different relationships to the OASPL. This is contrary to D_{eq} which is proportional to $(hw)^{1/2}$. Figure 19 is the same data shown in the previous figures, however it has now been scaled using the previously defined L_{eq}. As can be seen from the figure, the data collapses reasonably well over much of the frequency range. Notice that L_{eq} is used to collapse the amplitude of the spectra (OASPL ~ L_{eq}^2) and also to non-dimensionalize the frequency ($f L_{eq}/V_j$) for different conditions.

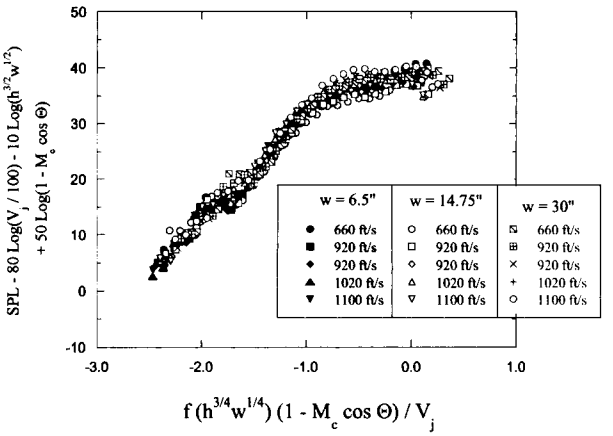

Figure 19: HARN acoustic spectra scaled by "best fit" to OASPL data, SPL ~ $V^8Leq^2(1 - Mccos\Theta)^{-5}$, $L_{eq} = h^{3/4}w^{1/4}$, $\Theta = 90°$

In figure 19 the frequency is non-dimensionalized into a Strouhal number based on L_{eq}. This is contrary to other researchers who have non-dimensionalized the frequency based on D_{eq} or h. Larsen performed an extensive adaptation of round jet noise theories to 2-d rectangular jets.[32, 33] He stated that h is the appropriate length scale for the axial and normal directions (x and y directions for the HARN) for a rectangular jet with AR >30. Tam and his colleagues[9, 26-27] state that D_{eq} is appropriate for the wide range of non-axisymmetric nozzles they have tested, including rectangular nozzles with aspect ratio up to about 10. The defined L_{eq} is not supported by any literature found by the authors, it is simply a combination of the trends seen in the data and the desire to stay dimensionally consistent with Lighthill's derivation where $I \sim L^2$. A theoretical basis for L_{eq} was explored in the references [29, 35, and 36] where attempts were made to develop a prediction scheme for rectangular jet noise based on

fluid dynamic experimental data and jet noise theories.

As in the case with OASPL, the previous few figures have shown data only for the $\Theta = 90^{\circ}$ case. This was done to be able to examine the effects of jet velocity, height and width on the spectra without the added complication of any effects due to convective amplification and refraction that is present at other polar angles. However, it is appropriate at this point to examine the data for polar angles other than 90°.

Figure 20 is an example of round jet data taken from reference [6]. Notice that there is large scatter at high frequencies. This is due to the differences seen between the data and Lighthill's prediction when examining the OASPL. Figure 21 shows similar results for the HARN data.

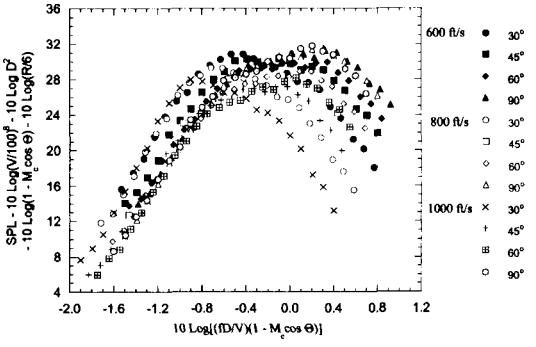

Figure 20: Round jet SPL spectra scaled according to Round jet theory for D = 2.4" from reference [6].

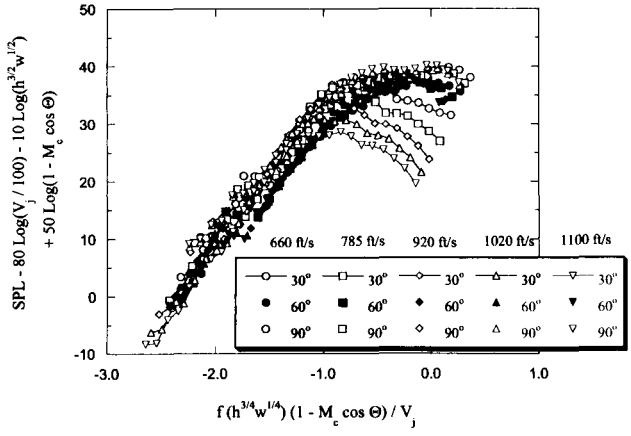

Figure 21: HARN SPL spectra scaled according to parameters developed

A further examination of the HARN noise data at various polar angles is warranted. Figure 22 shows data for the same test points as shown in figure 21 at some other polar angles. At $\Theta = 20^{\circ}$ there is very little collapse of the data except at the extremely low frequencies. As the jet velocity is increased, there is increasing scatter amongst the conditions. However, notice that data for similar velocities and polar angles tend to be grouped together. This indicates that at $\Theta = 20^{\circ}$ the relationship for L_{eq} is reasonable for constant jet velocity and polar angle. The data at $\Theta = 40^{\circ}$ shows a similar result, however to a lesser degree, and the 60° data shows reasonable collapse for each set of points of constant width, however there is some difference for different widths. Also, as expected, there is some scatter at lower frequencies caused by the low frequency peak that is believed to be due to internal noise.

APPENDIX C

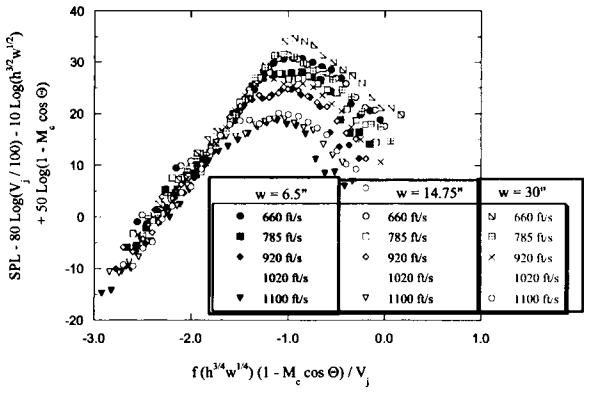

(a)

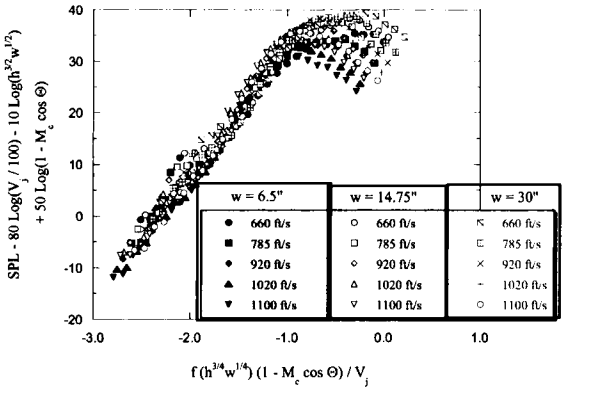

(b)

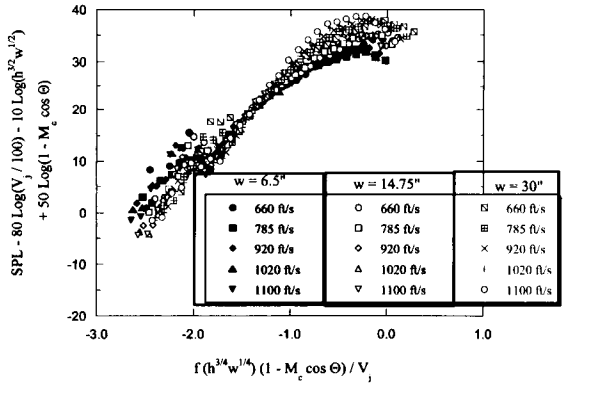

(c)

Figure 22: HARN SPL scaled according to parameters found using OASPL, (a) $\Theta = 20^\circ$, (b) $\Theta = 40^\circ$, (c) $\Theta = 60^\circ$.

Summary and Conclusions

A large amount of acoustic data was collected for the HARN. This included a range of aspect ratios from 100 to 3000, well above the range of rectangular jet noise data found in the literature. The jet velocities tested ranged from 400 to 1100 ft/s and data were recorded at 9 different polar angles.

The HARN acoustic data were compared with trends expected from Lighthill's theoretical predictions and those that are commonly used to collapse and scale round jet noise data and low-aspect-ratio rectangular jet noise data. An initial comparison of sample HARN and round nozzle data showed some general similarities, but also some distinct differences. The general shape of the spectra at various polar angles seemed to be similar. The directivity of the HARN noise seems to have a peak at about $\Theta = 20^\circ$, similar to what has been found for round jets. The HARN data also appeared to have a significant amount turbulent absorption and scattering of high frequency noise at low polar angles evidenced by lower SPL levels at high frequencies and higher SPLs at low frequencies for low polar angles.

From the HARN acoustic data, parameters for scaling acoustic data from a high aspect-ratio nozzle were found. The largest width data was found to vary with h^2 while the data for the two smaller nozzle widths were proportional to $h^{3/2}$. The width had only a moderate effect on the jet noise. Although no exact scaling relationship was extracted from the data, a best fit to the data was found to be $I \sim V_j^8 L_{eq}^2$, where $L_{eq} = h^{3/4} w^{1/4}$. The frequency was found to be weakly dependent on the nozzle height and width. Again, using a best-fit approach, and using the defined equivalent length as a normalizing parameter, the frequency was converted to Strouhal number by fL_{eq}/V_j. This definition came from the examination of the data and determining a best fit scaling law, while consistency with round jet noise theories and prediction schemes were used as a constraint, i.e., the sound intensity had to remain proportional to a characteristic length squared.

No direct relationship was found that provided reasonable scaling as a function of the polar angle. A first attempt to scale the data as a function of polar angle as it appears in the convective amplification term in Lighhill's formulation and subsequently modified by Ffowcs-Williams. This formulation did not work well at smaller polar angles. However, this result was similar to what other researchers have found when applying it to round jet noise data. It is believed that this is due to scattering and absorption of turbulence that must pass through the shear layer of the jet on its path to a microphone at a low polar angle.

APPENDIX C

Acknowledgments

This work was sponsored by NASA Grant-NAG1-2146 through NASA Langley, under its Breakthrough Innovative Technology Program. Thanks are also due to Mr. C. Jameson for designing the HARN nozzle and to Drs. Rick Gaeta and Kevin Massey of GTRI for their assistance in the experiments and many useful discussions.

References

1. Lighthill, M.J. "On sound Generated Aerodynamically. I. General Theory," Proceedings of the Royal Society A 211, pp 564-578, 1952.
2. Lighthill, M.J. "On sound Generated Aerodynamically. II. Turbulence as a Source of Sound," Proceedings of the Royal Society A 222, pp 1-21, 1954.
3. Lighthill, M.J. "Jet Noise," North Atlantic Treaty Organization Advisory Group for Aeronautical Research and Development, Report 448, 1963.
4. Lush, P. A., "Measurements of Subsonic Jet Noise and Comparison with Theory," Journal of Fluid Mechanics, Vol. 46, part 3, pp.477-500,1971.
5. Ahuja, K.K. "Correlation and Prediction of Jet Noise," Journal of Sound and Vibration, 29 (2), pp 155-168, 1973.
6. Ahuja, K.K., and Bushell, K.W. "An Experimental Study of Subsonic Jet Noise and Comparison with Theory," Journal of Sound and Vibration, 30 (3), pp 317-341. 1973.
7. Tam, Christopher K.W., Auriault, Laurent, "Jet Mixing Noise from Fine Scale Turbulence." AIAA Paper 98-2354, 1998.
8. Tam, C.K.W., Golebiowski, M., and Seiner, J.M., "On the Two components of turbulent Mixing Noise from Supersonic Jets." AIAA Paper 96-1716, 1996.
9. Tam, Christopher K. W., and Pastouchenko, Nikolai, "Noise from the Fine Scale Turbulence of Nonaxisymmetric Jets." AIAA Paper 2001-2187, May 2001.
10. Tam, Christopher K. W., "On the Failure of the Acoustic Analogy theory to Identify the Correct Noise Sources." AIAA Paper 2001-2117, May 2001.
11. Tyler, J. M., Sofrin, T. G., Davis, J. W., "Rectangular Nozzles for Jet Noise Suppression," SAE National Aeronautic Meeting, April 1959.
12. Capone, F. J., and Maiden, D. L., "Performance of Twin Two-Dimensional Wedge Nozzles Including Thrust Vectoring and Reversing Effects at Speeds up to Mach 2.20," NASA TN D-8449, 1977.
13. Capone, F. J., Hunt, B. L., and Path, G. E., "Subsonic/Supersonic Nonvectored Aeropropulsive Characteristics of Nonaxisymmetric Nozzles Installed on an F-18 Model." AIAA Paper 81-1445. 1981.
14. Seiner, John M., Ponton, Michael K., Manning, James C., "Acoustic Properties Associated with Rectangular Geometry Supersonic Nozzles," AIAA Paper 86-1472, 1986.
15. Kouts, C. A., and Yu, J. C., "Far Noise Field of a Two-Dimensional Subsonic Jet." AIAA Journal Vol. 3, No. 8, pp. 1031 – 1035. August 1975.
16. Maglieri, D. J., and Hubbard, H. H., "Preliminary Measurements of the Noise Characteristics of Some Jet Augmented Flap Configurations." NASA Memo 12-4-58L, 1958.
17. Coles, W. D., "Jet Engine Exhaust from Slot Nozzles." NASA TN D-60, 1959.
18. Maestrello, L., and McDaid, E., "Acoustic Characteristics of a High-Subsonic Jet." AIAA Journal, Vol. 9, No. 6, pp. 1058-1066, 1971.
19. Gruschka, H. D., and Schrecker, G. O., "Aeroacoustic Characteristics of Jet Flap Type Exhausts." AIAA Paper 72-130, 1972.
20. Schrecker, G. O., and Maus, J. R., "Noise Characteristics of Jet Flap Type Exhaust Flows." NASA Grant, NGR 43-001-075, 1975.
21. Olsen, W. A., Butierrez, O., and Dorsch, R. G., "The Effect of Nozzle Inlet Shape, Lip Thickness, and Exit Shape and Size on Subsonic Jet Noise." AIAA Paper 73-187, 1973.
22. Ffowcs-Williams, J. E., "Some Open Questions on the Jet Noise Problem." Boeing Science research Lab. Doc., DL-82-0730, 1968.
23. von Glahn, U. H., "Rectangular Nozzle Plume Velocity Modeling for use in Jet Noise Prediction." AIAA Paper 89-2357, 1989.
24. Tam, Christopher K. W., and Zaman, K. B. M. Q., "Subsonic Jet Noise from Nonaxisymmetric and Tabbed Nozzles." AIAA Journal, Vol. 38, No. 4, pp. 592-599, April 2000.
25. Tam, Christopher K. W., "Influence of Nozzle Geometry on the Noise of High-Speed Jets." AIAA Journal, Vol. 36, No. 8, pp. 1396-1400, August 1998.
26. Tam, C.K.W. and Zaman, K.B.M.Q., "Subsonic Jet Noise from Non-Axisymmetric and Tabbed Nozzles." AIAA Paper 99-0077, 1999.
27. Tam, Christopher K.W., "Influence of Nozzle Geometry on the Noise of High Speed Jets." AIAA paper 98-2255, 1998.
28. Munro, Scott E., Ahuja, K. K., and Englar R. J., "Airframe Noise Reduction Through Pneumatic Technology: Experiments." Submitted for

Publication to Journal of Aircraft, February, 2002.

29. Munro, Scott Edward, "Jet Noise of High Aspect-Ratio Rectangular Nozzles with Application to Pneumatic High-Lift Devices." Georgia Institute of Technology, PhD thesis, January, 2002.
30. Pope, Alan, Wind Tunnel Testing. 2nd Ed. John Wiley & Sons, NY, pp 31-80, 1964.
31. Ahuja, K.K., Tanna, H.K., and Tester, B.J. "An experimental Study of Transmission, Reflection and Scattering of Sound in A Free Jet Flight Simulation Facility and Comparison with Theory," Journal of Sound and Vibration, 75 (1), pp 51-85, 1981
32. Larsen, P. N., "Noise Generated by Air Jets from a Rectangular Slit." Ph.D. Thesis, Technical University of Denmark, 1983.
33. Bjorno, L, and Larsen, P. N., "Noise of Jets from Rectangular Slits." Acoustica, Vol. 54, pp. 247 – 256, 1984.
34. Ffowcs Williams, J.E., "The Noise From Turbulence Convected at High Speed." Philosophical Transactions of the royal Society, Vol. A-255, pp. 469-503, 1963.
35. Munro, Scott E. and Ahuja, K. K., "Fluid Dynamics of a High Aspect- Ratio Jet," AIAA-2003-3129, 2003, presented at the 9th AIAA/CEAS Aeroacoustics Conference and Exhibit, Hilton Head, South Carolina, USA, 12 - 14 May 2003.
36. Munro, Scott E. and Ahuja, K. K., "Development of a Prediction Scheme for Noise of High-Aspect Ratio Jets," AIAA-2003-3255, 2003, presented at the 9th AIAA/CEAS Aeroacoustics Conference and Exhibit, Hilton Head, South Carolina, USA, 12 - 14 May 2003.